

Molybdenum and Tungsten Complexes of Sulfene (Thioformaldehyde *S,S*-Dioxide)¹

Wolfdieter A. Schenk,* Katja Nielsen, Nicolai I. Burzlaff,† and Michael Hagel

Institut für Anorganische Chemie, Universität Würzburg, Am Hubland,
D-97074 Würzburg, Germany

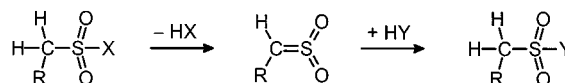
Received September 10, 2001

Propionitrile complexes *fac*-[M(CO)₃(P-P)(NCEt)] (M = Mo (**3**), W (**4**); P-P = Ph₂PCH₂PPh₂ (**a**), Ph₂PC₂H₄PPh₂ (**b**), Ph₂PC₃H₆PPh₂ (**c**), (*S,S*)-Ph₂PCHMeCHMePPh₂ (**d**), Fe(C₅H₄PPh₂)₂ (**e**)) were synthesized from [M(CO)₃(NCEt)₃] and the corresponding diphosphine. Reactions of **3** and **4** with sulfur dioxide initially gave complexes *fac*-[M(CO)₃(P-P)(η^2 -SO₂)] (M = Mo (**5**), W (**6**)), which slowly isomerized to *mer*-[M(CO)₃(P-P)(η^1 -SO₂)] (M = Mo (**7**), W (**8**)). The structures of **7b** and **8b** were determined by X-ray crystallography. Both compounds are isostructural (monoclinic, space group *P*₂₁/*n* (No. 14)) with almost identical unit cell dimensions (**7b**, *a* = 14.511(5) Å, *b* = 12.797(2) Å, *c* = 16.476(6) Å, β = 115.92(2)°; **8b**, *a* = 14.478(8) Å, *b* = 12.794(3) Å, *c* = 16.442(9) Å, β = 116.01(2)°) and molecular geometries. Treatment of either *fac*-[M(CO)₃(P-P)(η^2 -SO₂)] or *mer*-[M(CO)₃(P-P)(η^1 -SO₂)] with diazomethane yielded the sulfene complexes *mer*-[M(CO)₃(P-P)(η^2 -CH₂SO₂)] (M = Mo (**9**), W (**10**)). The structure of **10a** was determined crystallographically: monoclinic, space group *P*₂₁/*n* (No. 14), *a* = 11.719(2) Å, *b* = 17.392(4) Å, *c* = 13.441(3) Å, β = 95.58(2)°. The tungsten atom resides in the center of a distorted pentagonal bipyramid. The sulfene ligand occupies two adjacent equatorial sites with the bond distances W–C, 2.322(13) Å, W–S, 2.353(3) Å, and S–C, 1.721(12) Å. The latter equals the S–C single bond distance in thiirane *S,S*-dioxide, indicating a high degree of charge density transfer into the LUMO of the sulfene ligand.

Introduction

Short-lived and highly reactive molecules can often be stabilized by coordination to a transition metal complex.² This provides an opportunity to gain structural and spectroscopic information not accessible by other means. In an ideal case the species under consideration is not only stabilized but sufficiently modified that it can undergo novel stoichiometric and perhaps even catalytic reactions. Transition metal complexes of carbenes are certainly the most prominent examples of this principle.³ Sulfenes R¹R²C=SO₂ are reactive intermediates that may be generated by 1,2-elimination or by cycloreversion reactions.⁴ They are involved in numerous transformations of derivatives of alkanesulfonic acids⁴

Scheme 1. Elimination–Addition Reactions of Sulfonic Acid Derivatives



(Scheme 1) as well as in the SO₂-catalyzed decomposition of diazo compounds^{4,5} (Scheme 2).

A limited number of sulfenes bearing highly electronegative substituents have been isolated as base adducts.⁶ The

* To whom correspondence should be addressed. E-mail: wolfdieter.schenk@mail.uni-wuerzburg.de. FAX (+49) (0)931-888-4605.

† Current address: Fachbereich Chemie, Universität Konstanz, Universitätsstrasse 10, D-78457 Konstanz, Germany.

(1) Sulfur(IV) Compounds as Ligands. 26. Part 25: El-khateeb, M.; Wolfsberger, B.; Schenk, W. A. *J. Organomet. Chem.* **2000**, *612*, 14–17.

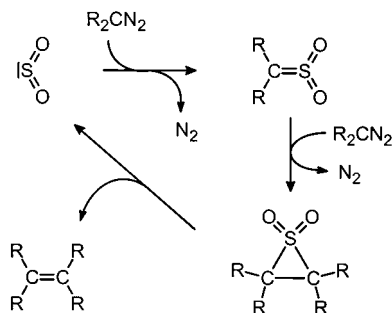
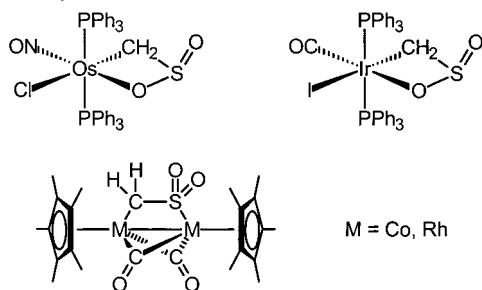
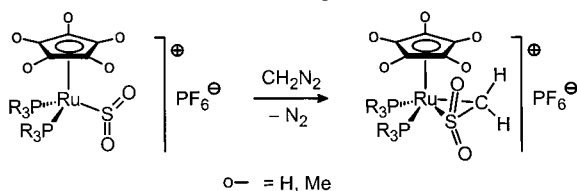
(2) Collman, C. P.; Hegedus, L. S.; Norton, J. R.; Finke, R. G. *Principles and Applications of Organotransition Metal Chemistry*; University Science Books: Mill Valley, 1987; pp 1–18.

(3) (a) Doyle, M. P. In *Comprehensive Organometallic Chemistry II*; Hegedus, L. S., Ed.; Pergamon: Oxford, 1995; Vol. 12, pp 387–420. (b) Wulff, W. D. In *Comprehensive Organometallic Chemistry II*; Hegedus, L. S., Ed.; Pergamon: Oxford, 1995; Vol. 12, pp 469–547. (c) Hegedus, L. S. In *Comprehensive Organometallic Chemistry II*; Hegedus, L. S., Ed.; Pergamon: Oxford, 1995; Vol. 12, pp 549–576. (d) Stille, J. R. In *Comprehensive Organometallic Chemistry II*; Hegedus, L. S., Ed.; Pergamon: Oxford, 1995; Vol. 12, pp 577–594.

(4) King, J. F.; Rathore, R. In *The Chemistry of Sulfonic Acids, Esters, and Their Derivatives*; Patai, S., Rappoport, Z., Eds.; Wiley: New York, 1991; pp 583–669.

(5) Staudinger, H.; Pfenninger, F. *Ber. Dtsch. Chem. Ges.* **1916**, *49*, 1941–1951.

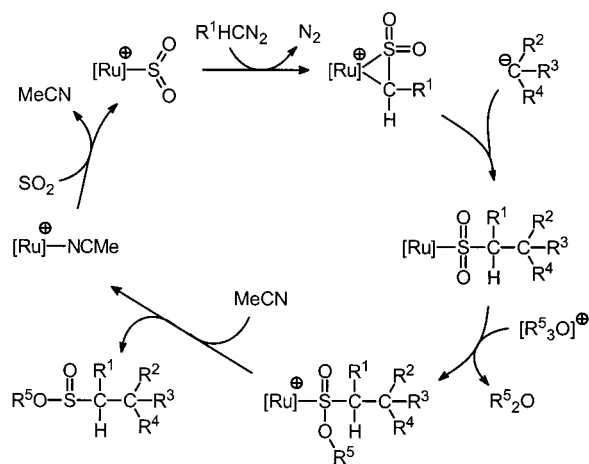
(6) (a) Hartwig, U.; Pritzkow, H.; Rall, K.; Sundermeyer, W. *Angew. Chem.* **1989**, *101*, 224–225; *Angew. Chem., Int. Ed. Engl.* **1989**, *28*, 221–222. (b) Sundermeyer, W. *Synthesis* **1988**, *5*, 349–359. (c) Opitz, G.; Ehliis, T.; Rieth, K. *Chem. Ber.* **1990**, *123*, 1989–1998.

Scheme 2. SO₂-Catalyzed Decomposition of Diazo Compounds**Scheme 3.** Mono- and Binuclear Complexes of Sulfene (Thioformaldehyde *S,S*-Dioxide)**Scheme 4.** Cationic Ruthenium Complexes of Sulfene

parent thioformaldehyde *S,S*-dioxide has been stabilized as a $\eta^2(S,O)$ ligand in two complexes of osmium⁷ and in some binuclear complexes of cobalt and rhodium⁸ (Scheme 3).

Cationic ruthenium complexes of the type $[(C_5H_5)(R_3P)_2-Ru\{\eta^2(S,C)-H_2C=SO_2\}]^+$ are readily accessible by methylene transfer to the corresponding sulfur dioxide complexes⁹ (Scheme 4).

This reaction exploits the pronounced electrophilicity of cationic complexes of sulfur dioxide.¹⁰ The products also turned out to be highly reactive electrophiles which readily add a variety of bases (amines, phosphines, halides).⁹ Furthermore, they undergo C–C coupling reactions with enamines and enolates leading ultimately to a transition metal mediated synthesis of esters of functionalized sulfinic acids¹¹ (Scheme 5).

Scheme 5. Synthesis of Sulfinic Acid Esters via Cationic Ruthenium–Sulfene Complexes

The work reported here was undertaken with the aim to investigate the reactivity of the neutral uncharged sulfur dioxide complexes $[M(CO)_3(P-P)(SO_2)]$ ($M = Mo, W$, ($P-P$) = chelating diphosphine)¹² toward the nucleophile diazomethane and to assess the structure and stability of the resulting sulfene complexes.

Experimental Section

Analytical Measurements. C, H, and S analyses were carried out by the Analytical Laboratory of the Institute of Inorganic Chemistry, University of Würzburg (due to carbide formation tungsten complexes occasionally analyze low for carbon). Melting points were determined by differential scanning calorimetry (DSC). Infrared spectra were run on a Bruker IFS 25 instrument. ¹H, ¹³C-¹H, and ³¹P{¹H} NMR spectra were recorded using a Bruker AMX 400 instrument. Chemical shifts were referenced to the internal solvent signals and are reported relative to TMS (¹H, ¹³C) or 85% H₃PO₄ (³¹P).

Materials. The propionitrile complexes $[M(CO)_3(NCEt)_3]$ ($M = Mo, W$) were obtained by refluxing the metal hexacarbonyls in propionitrile.¹³ The diphosphines were obtained from Strem Chemicals and were used as received. The phosphine–nitrile complexes **3a,b** and **4a,b**^{12,14} and the sulfur dioxide complexes **7b** and **8b**¹² were obtained by published procedures or slight adaptations thereof. Sulfur dioxide was dried by passing it through concentrated sulfuric acid. Diazomethane was prepared from *N*-methyl-*N*-nitroso-4-toluenesulfonamide and employed as a dilute solution in ether.

Propionitrile Complexes 3c–e and 4c–e. General Procedure. $[M(CO)_3(NCEt)_3]$ (2.00 mmol) and diphosphine (2.00 mmol) were suspended in propionitrile (40 mL). The flask was immersed for 5 min into an ultrasonic cleaning bath in order to disperse the starting complex, and stirred at 20 °C for 1 h ($M = Mo$) or 8 h ($M = W$), respectively. Ether (40 mL) was added to precipitate the products, which were then filtered off, washed with ether (40 mL), and dried under vacuum.

- (7) Roper, W. R.; Waters, J. M.; Wright, A. H. *J. Organomet. Chem.* **1984**, *276*, C13–C15.
 (8) (a) Herrmann, W. A.; Bauer, C. *Organometallics* **1982**, *1*, 1101–1102. (b) Herrmann, W. A.; Bauer, C.; Weichmann, J. *Chem. Ber.* **1984**, *117*, 1271–1268.
 (9) (a) Schenk, W. A.; Urban, P. *J. Organomet. Chem.* **1991**, *411*, C27–C31. (b) Schenk, W. A.; Urban, P.; Dombrowski, E. *Chem. Ber.* **1993**, *126*, 679–684.
 (10) (a) Schenk, W. A.; Karl, U. *Z. Naturforsch., B* **1989**, *44*, 993–995. (b) Schenk, W. A.; Urban, P.; Stähfeldt, T.; Dombrowski, E. *Z. Naturforsch., B* **1992**, *47*, 1493–1500.
 (11) (a) Schenk, W. A.; Bezler, J. *Eur. J. Inorg. Chem.* **1998**, 605–611. (b) Schenk, W. A.; Bezler, J.; Burzlaff, N.; Hagel, M.; Steinmetz, B. *Eur. J. Inorg. Chem.* **2000**, 287–297.

- (12) (a) Schenk, W. A.; Baumann, F.-E. *Chem. Ber.* **1982**, *115*, 2615–2625. (b) Schenk, W. A.; Baumann, F.-E. *J. Organomet. Chem.* **1983**, *256*, 261–267. (c) Kubas, G. J.; Jarvinen, G. D.; Ryan, R. R. *J. Am. Chem. Soc.* **1983**, *105*, 1883–1891.
 (13) Kubas, G. J.; van der Sluys, L. S. *Inorg. Synth.* **1990**, *28*, 29–33.
 (14) (a) Darensbourg, D. J.; Zalewski, D. J.; Plepys, C.; Campana, C. *Inorg. Chem.* **1987**, *26*, 3727–3732. (b) Hsu, S. C. N.; Yeh, W. Y.; Chiang, M. Y. *J. Organomet. Chem.* **1995**, *492*, 121–127. (c) Song, L.-C.; Liu, J.-T.; Hu, Q.-M.; Wang, G.-F.; Zanello, P.; Fontani, M. *Organometallics* **2000**, *19*, 5342–5351.

(a) **[Mo(CO)₃(dppp)(NCEt)], 3c**: yield 93%, yellow crystalline powder, mp 71 °C (dec). Anal. Calcd for C₃₃H₃₁MoNO₃P₂: C, 61.21; H, 4.83; N, 2.16. Found: C, 60.82; H, 4.69; N, 2.23. IR (CH₂Cl₂): $\nu(\text{CO})$ 1934 (vs), 1842 (s), 1811 (s) cm⁻¹. ³¹P NMR (CD₂Cl₂): δ 22.0 (s).

(b) **[Mo(CO)₃(chir)(NCEt)], 3d**: yield 95%, yellow crystalline powder, mp 140 °C (dec). Anal. Calcd for C₃₄H₃₃MoNO₃P₂: C, 61.73; H, 5.03; N, 2.12. Found: C, 61.59; H, 5.02; N, 2.22. IR (CH₂Cl₂): $\nu(\text{CO})$ 1934 (vs), 1843 (s), 1811 (s) cm⁻¹. ³¹P NMR (CD₂Cl₂): δ 59.7 (d, *J*(P,P) = 7 Hz), 63.4 (d, *J*(P,P) = 7 Hz).

(c) **[Mo(CO)₃(dppf)(NCEt)], 3e**: yield 87%, dark yellow crystalline powder, mp 98 °C (dec). Anal. Calcd for C₄₀H₃₃FeMoNO₃P₂: C, 60.86; H, 4.21; N, 1.77. Found: C, 60.39; H, 4.34; N, 1.63. IR (CH₂Cl₂): $\nu(\text{CO})$ 1932 (vs), 1837 (s), 1809 (s) cm⁻¹. ³¹P NMR (CD₂Cl₂): δ 30.5 (s).

(d) **[W(CO)₃(dppp)(NCEt)], 4c**: yield 59%, yellow crystalline powder, mp 78 °C (dec). Anal. Calcd for C₃₃H₃₁NO₃P₂W: C, 53.90; H, 4.25; N, 1.90. Found: C, 53.52; H, 4.09; N, 1.99. IR (CH₂Cl₂): $\nu(\text{CO})$ 1911 (vs), 1831 (s), 1809 (s) cm⁻¹. ³¹P NMR (CD₂Cl₂): δ 7.6 (s, *J*(W,P) = 220 Hz).

(e) **[W(CO)₃(chir)(NCEt)], 4d**: yield 84%, yellow crystalline powder, mp 151 °C (dec). Anal. Calcd for C₃₄H₃₃NO₃P₂W: C, 54.49; H, 4.44; N, 1.87. Found: C, 54.05; H, 4.31; N, 1.92. IR (CH₂Cl₂): $\nu(\text{CO})$ 1924 (vs), 1831 (s), 1816 (s) cm⁻¹. ³¹P NMR (CD₂Cl₂): δ 49.0 (d, *J*(P,P) = 3 Hz, *J*(W,P) = 225 Hz), 53.3 (d, *J*(P,P) = 3 Hz, *J*(W,P) = 225 Hz).

(f) **[W(CO)₃(dppf)(NCEt)], 4e**: yield 64%, dark yellow crystalline powder, mp 68 °C (dec). Anal. Calcd for C₄₀H₃₃FeNO₃P₂W: C, 54.76; H, 3.79; N, 1.60. Found: C, 54.17; H, 3.98; N, 1.76. IR (CH₂Cl₂): $\nu(\text{CO})$ 1927 (vs), 1831 (s), 1809 (s) cm⁻¹. ³¹P NMR (CD₂Cl₂): δ 21.5 (s, *J*(W,P) = 233 Hz).

Sulfur Dioxide Complexes. General Procedure. [M(CO)₃(P-P)(NCEt)] (0.50 mmol) was suspended in dichloromethane (20 mL) and the solution saturated at 0 °C with SO₂. The mixture turned red immediately and was stirred for 2 h at 0 °C and then for 24 h at 20 °C. Excess SO₂ and solvent were removed by partial evaporation, and the product was precipitated by addition of hexane (40 mL).

(a) **fac-[W(CO)₃(dppf)(SO₂)], 6e**: yield 71%, purple crystalline powder, mp 54 °C (dec). Anal. Calcd for C₃₇H₂₈FeO₅P₂SW: C, 50.14; H, 3.18; S, 3.62. Found: C, 49.51; H, 3.53; S, 3.30. IR (CH₂Cl₂): $\nu(\text{CO})$ 1985 (vs), 1894 (s) cm⁻¹. IR (Nujol): $\nu(\text{SO})$ 1145 (s), 997 (w) cm⁻¹. ³¹P NMR (CD₂Cl₂): δ 8.0 (d, *J*(P,P) = 29 Hz, *J*(W,P) = 220 Hz), 16.0 (d, *J*(P,P) = 29 Hz, *J*(W,P) = 217 Hz).

(b) **mer-[Mo(CO)₃(dppm)(SO₂)], 7a**: yield 52%, bright red crystalline powder, mp 141 °C (dec). Anal. Calcd for C₂₈H₂₂MoO₅P₂S: C, 53.52; H, 3.53; S, 5.10. Found: C, 52.94; H, 3.59; S, 4.93. IR (CH₂Cl₂): $\nu(\text{CO})$ 2012 (w), 1960 (sh), 1935 (vs) cm⁻¹. IR (Nujol): $\nu(\text{SO})$ 1220 (w), 1061 (s) cm⁻¹. ³¹P NMR (CD₂Cl₂): δ -3.1 (s), 0.8 (s).

(c) **mer-[Mo(CO)₃(dppp)(SO₂)], 7c**: yield 45%, bright red crystalline powder, mp 67 °C (dec). Anal. Calcd for C₃₀H₂₆MoO₅P₂S: C, 54.89; H, 3.99; S, 4.88. Found: C, 55.17; H, 3.98; S, 4.33. IR (CH₂Cl₂): $\nu(\text{CO})$ 2014 (w), 1954 (sh), 1918 (vs) cm⁻¹. IR (Nujol): $\nu(\text{SO})$ 1234 (w), 1069 (s) cm⁻¹. ³¹P NMR (CD₂Cl₂): δ 13.9 (d, *J*(P,P) = 38 Hz), 24.3 (d, *J*(P,P) = 38 Hz).

(d) **mer-[Mo(CO)₃(chir)(SO₂)], 7d**: yield 60%, bright red crystalline powder, mp 61 °C (dec). Anal. Calcd for C₃₁H₂₈MoO₅P₂S: C, 55.53; H, 4.21; S, 4.78. Found: C, 55.31; H, 4.57; S, 4.50. IR (CH₂Cl₂): $\nu(\text{CO})$ 2018 (w), 1955 (sh), 1928 (vs) cm⁻¹. IR (Nujol): $\nu(\text{SO})$ 1238 (w), 1065 (s) cm⁻¹. ³¹P NMR (CD₂Cl₂): δ 61.7 (d, *J*(P,P) = 23 Hz), 65.1 (d, *J*(P,P) = 23 Hz).

(e) **mer-[W(CO)₃(dppm)(SO₂)], 8a**: yield 54%, bright red crystalline powder, mp 146 °C (dec). Anal. Calcd for C₂₈H₂₂O₅P₂SW: C, 46.95; H, 3.10; S, 4.48. Found: C, 46.22; H, 3.05; S, 4.21. IR (CH₂Cl₂): $\nu(\text{CO})$ 2021 (w), 1950 (m), 1922 (vs) cm⁻¹. IR (Nujol): $\nu(\text{SO})$ 1211 (w), 1059 (s) cm⁻¹. ³¹P NMR (CD₂Cl₂): δ -28.6 (d, *J*(P,P) = 6 Hz, *J*(W,P) = 213 Hz), -27.6 (d, *J*(P,P) = 6 Hz, *J*(W,P) = 208 Hz).

(f) **mer-[W(CO)₃(dppp)(SO₂)], 8c**: yield 82%, bright red crystalline powder, mp 126 °C (dec). Anal. Calcd for C₃₀H₂₆O₅P₂SW: C, 48.41; H, 3.52; S, 4.31. Found: C, 48.80; H, 3.64; S, 3.99. IR (CH₂Cl₂): $\nu(\text{CO})$ 2018 (w), 1951 (m), 1919 (vs) cm⁻¹. IR (Nujol): $\nu(\text{SO})$ 1229 (w), 1068 (s) cm⁻¹. ³¹P NMR (CD₂Cl₂): δ -4.7 (d, *J*(P,P) = 30 Hz, *J*(W,P) = 224 Hz), 2.1 (d, *J*(P,P) = 30 Hz, *J*(W,P) = 244 Hz).

(g) **mer-[W(CO)₃(chir)(SO₂)], 8d**: yield 87%, bright red crystalline powder, mp 90 °C (dec). Anal. Calcd for C₃₁H₂₈O₅P₂SW: C, 49.09; H, 3.72; S, 4.23. Found: C, 48.81; H, 3.85; S, 3.81. IR (CH₂Cl₂): $\nu(\text{CO})$ 2015 (w), 1949 (m), 1916 (vs) cm⁻¹. IR (Nujol): $\nu(\text{SO})$ 1237 (w), 1070 (s) cm⁻¹. ³¹P NMR (CD₂Cl₂): δ 45.9 (d, *J*(P,P) = 12 Hz, *J*(W,P) = 250 Hz), 46.6 (d, *J*(P,P) = 12 Hz, *J*(W,P) = 231 Hz).

The *fac* isomers **5d** and **6d,e** were obtained as purple crystalline compounds when the reaction was worked up after 2 h at 0 °C. They were contaminated with 10–25% of the corresponding *mer* isomers, but further purification was not attempted.

(h) **fac-[Mo(CO)₃(chir)(SO₂)], 5d**. IR (CH₂Cl₂): $\nu(\text{CO})$ 1996 (vs), 1924 (s), cm⁻¹. IR (Nujol): $\nu(\text{SO})$ 1158 (m), 997 (w) cm⁻¹. ³¹P NMR (CD₂Cl₂): δ 46.2 (d, *J*(P,P) = 19 Hz), 58.1 (d, *J*(P,P) = 19 Hz).

(i) **fac-[W(CO)₃(dppp)(SO₂)], 6c**. IR (CH₂Cl₂): $\nu(\text{CO})$ 1993 (m), 1909 (s) cm⁻¹. IR (Nujol): $\nu(\text{SO})$ 1152 (m), 968 (w) cm⁻¹. ³¹P NMR (CD₂Cl₂): δ -0.9 (d, *J*(P,P) = 28 Hz), -0.4 (d, *J*(P,P) = 28 Hz).

(j) **fac-[W(CO)₃(chir)(SO₂)], 6d**. IR (CH₂Cl₂): $\nu(\text{CO})$ 1991 (m), 1909 (s) cm⁻¹. IR (Nujol): $\nu(\text{SO})$ 1155 (m), 989 (w) cm⁻¹. ³¹P NMR (CD₂Cl₂): δ 32.7 (d, *J*(P,P) = 9 Hz), 48.1 (d, *J*(P,P) = 9 Hz).

Sulfene Complexes. General Procedure. [M(CO)₃(P-P)(SO₂)] (0.20 mmol) was suspended in dichloromethane (10 mL), and a solution of diazomethane (1.0 mmol) in ether was added at 0 °C. The reactions were accompanied by gas evolution and a quick color change to yellow. Excess diazomethane and solvent were removed by evaporation to a volume of 2 mL. The products were precipitated by slow addition of ether (10 mL) and hexane (20 mL).

(a) **mer-[Mo(CO)₃(dppm)(CH₂SO₂)], 9a**: yield 71%, beige crystalline powder, mp 74 °C (dec). Anal. Calcd for C₂₉H₂₄MoO₅P₂S: C, 54.22; H, 3.77; S, 4.99. Found: C, 54.24; H, 3.93; S, 4.91. IR (CH₂Cl₂): $\nu(\text{CO})$ 2037 (m), 1987 (m), 1939 (vs) cm⁻¹. IR (Nujol): $\nu(\text{SO})$ 1207 (w), 1097 (s) cm⁻¹. ¹H NMR (CDCl₃): δ 1.23 (broad s, SCH₂), 4.38 (t, *J*(P,H) = 9.2 Hz, PCH₂), 7.4–8.0 (m, Ph). ¹³C NMR (CD₂Cl₂): δ -7.1 (m, SCH₂), 42.1 (t, *J*(P,C) = 21 Hz, PCH₂), 131.6–134.5 (m, Ph), 208.9–209.7 (m, CO). ³¹P NMR (CD₂Cl₂): δ -11.6 (d, *J*(P,P) = 32 Hz), -5.6 (d, *J*(P,P) = 32 Hz).

(b) **mer-[Mo(CO)₃(dppe)(CH₂SO₂)], 9b**: yield 72%, beige crystalline powder, mp 68 °C (dec). Anal. Calcd for C₃₀H₂₆MoO₅P₂S: C, 54.89; H, 3.99; S, 4.88. Found: C, 54.62; H, 3.80; S, 4.93. IR (CH₂Cl₂): $\nu(\text{CO})$ 2035 (m), 1979 (m), 1938 (vs) cm⁻¹. IR (Nujol): $\nu(\text{SO})$ 1227 (w), 1092 (s) cm⁻¹. ¹H NMR (CDCl₃): δ 1.14 (d, *J*(P,H) = 2.0 Hz, SCH₂), 2.65–2.77 (m, PCH₂), 7.4–7.7 (m, Ph). ¹³C NMR (CD₂Cl₂): δ -10.9 (m, SCH₂), 28.6–

29.3 (m, PCH₂), 129.2–135.4 (m, Ph), 207.0–207.2 (m, CO). ³¹P NMR (CDCl₃): δ 56.0 (d, *J*(P,P) = 27 Hz), 60.1 (d, *J*(P,P) = 27 Hz).

(c) *mer*-[Mo(CO)₃(chir)(CH₂SO₂)], **9d**: yield 29%, beige crystalline powder, mp 54 °C (dec). This compound was not obtained in analytically pure form. IR (CH₂Cl₂): ν(CO) 2037 (w), 1973 (m), 1927 (vs) cm⁻¹. IR (Nujol): ν(SO) 1212 (vw), 1091 (m) cm⁻¹. ¹H NMR (CD₂Cl₂): δ 0.98 (m, CH₃), 2.35–2.52 (m, PCH), 7.2–7.7 (m, Ph). ¹³C NMR (CD₂Cl₂): δ -8.3 (m, SCH₂), 15.1 (dd, *J*(P,C) = 22 Hz, *J*(P,C) = 5 Hz, CH₃), 15.5 (dd, *J*(P,C) = 21 Hz, *J*(P,C) = 5 Hz, CH₃), 37.0–37.6 (m, PCH), 127.0–135.4 (m, Ph). ³¹P NMR (CD₂Cl₂): δ 63.0 (d, *J*(P,P) = 38 Hz), 64.6 (d, *J*(P,P) = 38 Hz).

(d) *mer*-[W(CO)₃(dppm)(CH₂SO₂)], **10a**: yield 96%, off-white crystalline powder, mp 118 °C (dec). Anal. Calcd for C₂₉H₂₄O₅P₂-SW: C, 47.69; H, 3.31; S, 4.39. Found: C, 47.53; H, 3.30; S, 4.38. IR (CH₂Cl₂): ν(CO) 2036 (m), 1978 (m), 1930 (vs) cm⁻¹. IR (Nujol): ν(SO) 1191 (w), 1097 (m) cm⁻¹. ¹H NMR (CDCl₃): δ 1.48 (broad s, SCH₂), 4.58 (t, *J*(P,H) = 10.0 Hz, PCH₂), 7.3–7.9 (m, Ph). ¹³C NMR (CD₂Cl₂): δ -12.7 (m, SCH₂), 40.8 (t, *J*(P,C) = 27 Hz, PCH₂), 129.3–133.8 (m, Ph), 199.8–199.9 (m, CO). ³¹P NMR (CDCl₃): δ -34.8 (d, *J*(P,P) = 26 Hz, *J*(W,P) = 199 Hz), -30.8 (d, *J*(P,P) = 26 Hz, *J*(W,P) = 171 Hz).

(e) *mer*-[W(CO)₃(dippe)(CH₂SO₂)], **10b**: yield 72%, off-white crystalline powder, mp 157 °C (dec). Anal. Calcd for C₃₀H₂₆O₅P₂-SW: C, 48.41; H, 3.52; S, 4.31. Found: C, 47.85; H, 3.59; S, 4.22. IR (CH₂Cl₂): ν(CO) 2031 (m), 1972 (m), 1921 (vs) cm⁻¹. IR (Nujol): ν(SO) 1201 (w), 1096 (m) cm⁻¹. ¹H NMR (CDCl₃): δ 1.36 (d, *J*(P,H) = 2.0 Hz, SCH₂), 2.72–2.83 (m, PCH₂), 7.4–7.7 (m, Ph). ¹³C NMR (CDCl₃): δ -16.0 (m, SCH₂), 20.5 (dd, *J*(P,C) = 29 Hz, *J*(P,C) = 15 Hz, PCH₂), 29.4 (dd, *J*(P,C) = 29 Hz, *J*(P,C) = 15 Hz, PCH₂), 129.3–133.4 (m, Ph), 199.4–199.6 (m, CO). ³¹P NMR (CDCl₃): δ 40.4 (d, *J*(P,P) = 18 Hz, *J*(W,P) = 199 Hz), 42.0 (d, *J*(P,P) = 18 Hz, *J*(W,P) = 198 Hz).

(f) *mer*-[W(CO)₃(dppp)(CH₂SO₂)], **10c**: yield 62%, off-white crystalline powder, mp 96 °C (dec). Anal. Calcd for C₃₁H₂₈O₅P₂-SW: C, 49.09; H, 3.72; S, 4.23. Found: C, 48.94; H, 3.86; S, 3.62. IR (CH₂Cl₂): ν(CO) 2021 (m), 1971 (m), 1908 (vs) cm⁻¹. IR (Nujol): ν(SO) 1205 (w), 1081 (m) cm⁻¹. ¹H NMR (CDCl₃): δ 0.98 (d, *J*(P,H) = 5.2 Hz, SCH₂), 2.05 (m, CH₂), 2.69–2.84 (m, PCH₂), 7.4–7.5 (m, Ph). ¹³C NMR (CD₂Cl₂): δ -9.0 (m, SCH₂), 18.1 (s, CH₂), 27.5 (dd, *J*(P,C) = 26 Hz, *J*(P,C) = 10 Hz, PCH₂), 29.2 (dd, *J*(P,C) = 27 Hz, *J*(P,C) = 9 Hz, PCH₂), 129.1–134.8 (m, Ph), 202.1–202.2 (m, CO), 207.7 (m, CO). ³¹P NMR (CD₂-Cl₂): δ -5.5 (d, *J*(P,P) = 40 Hz, *J*(W,P) = 173 Hz), -4.4 (d, *J*(P,P) = 40 Hz, *J*(W,P) = 192 Hz).

(g) *mer*-[W(CO)₃(chir)(CH₂SO₂)], **10d**: yield 69%, off-white crystalline powder, mp 107 °C (dec). Anal. Calcd for C₃₂H₃₀O₅P₂-SW: C, 49.76; H, 3.91; S, 4.15. Found: C, 48.46; H, 4.02; S, 3.90. IR (CH₂Cl₂): ν(CO) 2033 (m), 1969 (m), 1916 (vs) cm⁻¹. IR (Nujol): ν(SO) 1211 (w), 1092 (m) cm⁻¹. ¹H NMR (CD₂Cl₂): δ 0.8–1.01 (m, SCH₂, CH₃), 2.38–2.51 (m, PCH), 7.4–7.7 (m, Ph). ¹³C NMR (CD₂Cl₂): δ 15.0 (vt, N = |*J*(P,C) + *J*(P',C)| = 23 Hz, CH₃), 30.1 (vt, N = |*J*(P,C) + *J*(P',C)| = 9 Hz, CH₃), 37.4–38.4 (m, PCH), 129.0–135.5 (m, Ph), 200.5–200.6 (m, CO). ³¹P NMR (-30 °C, CD₂Cl₂): δ 45.8 (d, *J*(P,P) = 28 Hz, *J*(W,P) = 186 Hz), 46.9 (d, *J*(P,P) = 28 Hz, *J*(W,P) = 180 Hz).

(h) *mer*-[W(CO)₃(dppf)(CH₂SO₂)], **10e**: yield 95%, yellow crystalline powder, mp 108 °C (dec). Anal. Calcd for C₃₈H₃₀FeO₅P₂-SW: C, 50.69; H, 3.36; S, 3.56. Found: C, 50.38; H, 3.51; S, 3.50. IR (CH₂Cl₂): ν(CO) 2028 (m), 1964 (m), 1910 (vs) cm⁻¹. IR (Nujol): ν(SO) 1217 (w), 1084 (m) cm⁻¹. ¹H NMR (CD₂Cl₂): δ 1.02 (d, *J*(P,H) = 6.4 Hz, SCH₂), 4.24–4.43 (m, C₅H₄), 7.4–7.7 (m, Ph). ¹³C NMR (CD₂Cl₂): δ -6.6 (m, SCH₂), 72.8 (vt, N =

Table 1. Crystallographic Data for **7b**, **8b**, and **10a**

	7b	8b	10a
empirical formula	C ₂₉ H ₂₄ MoO ₅ P ₂ S	C ₂₉ H ₂₄ O ₅ P ₂ SW	C ₂₉ H ₂₄ O ₅ P ₂ SW
fw	642.46	730.37	730.37
temp, K	293	293	193
space group	<i>P</i> 2 ₁ / <i>n</i> (No. 14)	<i>P</i> 2 ₁ / <i>n</i> (No. 14)	<i>P</i> 2 ₁ / <i>n</i> (No. 14)
<i>a</i> , Å	14.511(5)	14.478(8)	11.719(2)
<i>b</i> , Å	12.797(2)	12.794(3)	17.392(4)
<i>c</i> , Å	16.476(6)	16.442(9)	13.441(3)
β, deg	115.92(2)	116.01(2)	95.58(3)
<i>V</i> , Å ³	2752(1)	2737(2)	2726.6(9)
<i>Z</i>	4	4	4
λ, Å	0.71073	0.70930	0.71073
ρ _{calcd} , g cm ⁻³	1.551	1.772	1.779
μ, cm ⁻¹	2.66	2.87	2.78
R1 [<i>I</i> > 2σ(<i>I</i>)]	0.044	0.0289	0.0749
wR2 [<i>I</i> > 2σ(<i>I</i>)] ^a	0.0648	0.0502	0.137

$$^a \text{wR2} = \{[\sum w(F_o^2 - F_c^2)^2] / [\sum w(F_o^2)^2]\}^{1/2}.$$

Table 2. Relevant Bond Distances (Å) and Angles (deg) for **7b**, **8b**, and **10a**

	7b (M = Mo)	8b (M = W)	10a (M = W)
M–S	2.254(1)	2.258(1)	2.353(3)
M–P(1)	2.509(1)	2.500(1)	2.490(3)
M–P(2)	2.531(1)	2.525(1)	2.498(3)
M–C(1)	2.030(4)	2.021(4)	2.008(12)
M–C(2)	2.024(4)	2.017(4)	2.017(14)
M–C(3)	2.045(4)	2.024(4)	2.010(13)
M–C(5)			2.322(13)
S–C(5)			1.721(12)
S–O(4)	1.442(3)	1.443(3)	1.438(10)
S–O(5)	1.430(4)	1.434(4)	1.499(9)
S–M–P(1)	177.89(4)	178.03(4)	160.28(10)
S–M–P(2)	100.96(4)	100.90(4)	92.38(10)
S–M–C(2)	90.12(11)	90.56(12)	116.3(4)
S–M–C(5)			43.2(3)
P(1)–M–P(2)	80.63(3)	80.58(4)	68.10(10)
P(1)–M–C(2)	88.31(11)	87.98(12)	83.3(4)
P(1)–M–C(5)			156.2(3)
P(2)–M–C(2)	168.90(11)	168.51(11)	151.1(4)
P(2)–M–C(5)			135.6(3)
C(1)–M–C(3)	176.5(2)	176.1(2)	173.1(5)
O(4)–S–O(5)	112.4(2)	112.3(2)	113.1(6)

|*J*(P,C) + *J*(P',C)| = 5 Hz, CH), 74.0 (d, *J*(P,C) = 6 Hz, CH), 74.3 (d, *J*(P,C) = 6 Hz, CH), 75.7 (d, *J*(P,C) = 5 Hz, CH), 75.9 (d, *J*(P,C) = 4 Hz, CH), 129.0–135.0 (m, Ph). ³¹P NMR (CD₂-Cl₂): δ 14.8 (d, *J*(P,P) = 36 Hz), 16.0 (d, *J*(P,P) = 36 Hz).

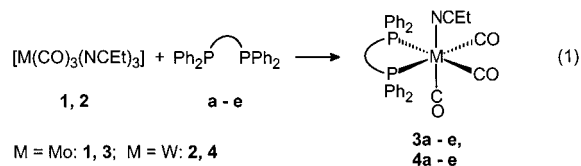
Crystallographic Studies of 7b, 8b, and 10a. Crystals were grown by diffusion of hexane into a dichloromethane solution of the complex. The data sets were collected on an Enraf-Nonius CAD4 using Mo Kα radiation. Empirical absorption corrections were applied.¹⁵ The structures were solved by Patterson methods with SHELXS-86.^{16a} The structures were refined by full-matrix least-squares procedures on *F*² using SHELXL-93.^{16b} All non-hydrogen atoms were refined anisotropically, and a riding model was employed in the refinement of the hydrogen atoms. Relevant crystallographic data can be found in Table 1, and selected bond distances and angles are given in Table 2. Further details on the structure investigations may be obtained from the Cambridge Crystallographic Data Centre on quoting the deposition numbers CCDC 165311 (**7b**), CCDC 165312 (**8b**), and CCDC 165313 (**10a**).

(15) North, A. C. T.; Phillips, D. C.; Mathews, F. S. *Acta Crystallogr.* **1968**, *A24*, 351–358.

(16) (a) Sheldrick, G. M. *Acta Crystallogr.* **1990**, *A46*, 467–473. (b) Sheldrick, G. M. Program for crystal structure refinement. University of Göttingen, 1993.

Results

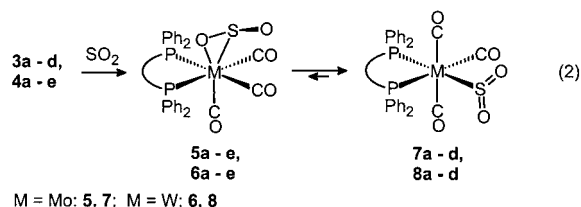
The tris(propionitrile) complexes **1** and **2** react smoothly with chelating diphosphines to produce the mixed-donor complexes **3a–e** and **4a–e** (eq 1).



	Ph ₂ P	PPh ₂
a	dppm	[Bis(diphenylphosphino)methane]
b	dppe	[1,2-Bis(diphenylphosphino)ethane]
c	dppp	[1,3-Bis(diphenylphosphino)propane]
d	chir	[2(S),3(S)-Bis(diphenylphosphino)butane]
e	dppf	[1,1'-Bis(diphenylphosphino)ferrocene]

Initially we had carried out this reaction in dichloromethane, which had led to products contaminated with varying amounts of the ligand-bridged dinuclear complexes [$\{\text{M}(\text{CO})_3(\text{P-P})\}_2(\mu\text{-P-P})$]. The use of propionitrile as a solvent slows the reaction down but makes it highly selective for the desired mononitrile complexes. Products **3a–e** and **4a–e** are yellow crystalline, slightly air-sensitive compounds. Their facial geometry as shown in eq 1 is easily inferred from the $\nu(\text{CO})$ pattern in the IR spectra and, with the exception of the chiral complexes **3d** and **4d**, the equivalence of the two phosphorus nuclei in the ³¹P NMR spectra. It should be mentioned here that closely analogous but somewhat less reactive acetonitrile complexes had been obtained in much the same way.^{12,14}

As had been noted earlier, phosphine–nitrile complexes of this type react instantaneously with sulfur dioxide.¹² IR monitoring indicated that initially the facial complexes **5a–e** and **6a–e** were formed which, with the exception of **5e** and **6e**, rearranged slowly to the meridional isomers (eq 2).



The formation of **5e** was only detected by IR spectroscopy; its low stability precluded isolation of a pure sample. Workup after short reaction times produced the facial isomers **5b,d** and **6b–e** in a sufficiently pure state for unambiguous spectroscopic identification. Since **5b** and **6b** had been isolated previously,¹² and since for the next step both isomers are equally suitable, we did not attempt a complete separation.

The facial isomers of the SO₂ complexes are deep burgundy-red or purple microcrystalline compounds while the meridional isomers are brick-red in color. They are soluble only in polar organic media such as dichloromethane, chloroform, or THF. The geometry around the central metal atom is unambiguously deduced from the relative intensity

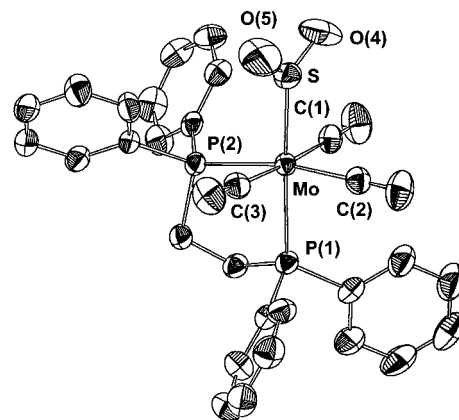


Figure 1. ORTEP plot of *mer*-[Mo(CO)₃(dppe)(SO₂)] (**7b**).

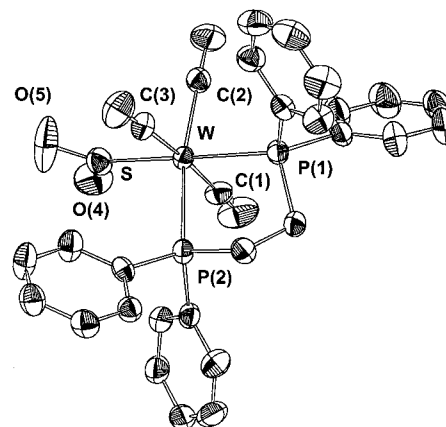


Figure 2. ORTEP plot of *mer*-[W(CO)₃(dppe)(SO₂)] (**8b**).

of the $\nu(\text{CO})$ absorptions, while the coordination mode of the sulfur dioxide ligand, $\eta^2(\text{S},\text{O})$ in the facial and $\eta^1(\text{S})$ in the meridional complexes, reveals itself through the readily identifiable SO stretching vibrations.¹⁷ The η^2 -(MSO₂) moiety is chiral, and as a result the two phosphorus nuclei in complexes **5** and **6** are diastereotopic. For **5d** and **6d** there is the possibility of the formation of diastereoisomers. However, only a single set of signals was observed in the ³¹P NMR spectra, indicating the highly preferential formation of one diastereoisomer.

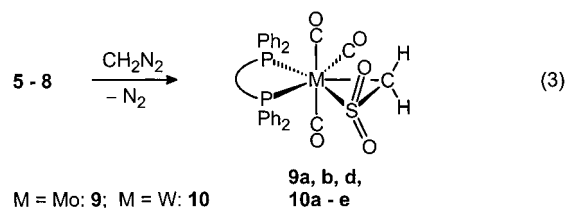
The structures of **7b** and **8b** were determined by X-ray crystallography; ORTEP diagrams are shown in Figures 1 and 2.

Both compounds are isostructural with almost identical unit cell data, and even the molecular dimensions of the two complexes are identical within 2σ . The structures are best described as slightly distorted octahedral. The largest deviation from the idealized geometry originates from the restraints imposed by the five-membered chelate ring which enforces a P–M–P angle of 80°. As a consequence, the corresponding P–M–S angle is opened up to 100°. The two M–P distances are, as expected, unequal due to the large structural *trans* influence of the strongly binding CO ligand.¹⁸ The M–S distances at 2.254 Å (M = Mo) and 2.258 Å (M = W) are

(17) (a) Kubas, G. J. *Inorg. Chem.* **1979**, *18*, 182–188. (b) Ryan, R. R.; Kubas, G. J.; Moody, D. C.; Eller, P. G. *Struct. Bonding* **1981**, *46*, 47–100.

between that in $[\text{Mo}(\text{CO})_3(\text{P-}i\text{-Pr}_3)_2(\text{SO}_2)]$ (2.285 Å), where the SO_2 ligand is situated *trans* to a CO,^{12c} and that in the more electron-rich $[\text{Mo}(\text{CO})_2(\text{dmpe})(\text{PPh}_3)(\text{SO}_2)]$ (2.244 Å), where the SO_2 is *trans* to one arm of the dmpe ligand.¹⁹ Thus it is clear that also the metal–sulfur distance depends on both the *trans* influence and the extent of π -bonding.

Treatment of the SO_2 complexes with diazomethane at 0 °C in each case gave a smooth reaction accompanied by gas evolution and a conspicuous color change to yellow. The resulting sulfene complexes were isolated as beige microcrystalline solids (eq 3).



The tungsten complexes are thermally more robust than their molybdenum congeners, which decompose rapidly in solution and even as solids have to be stored at -70 °C. The presence of the sulfene ligand was diagnosed by a doublet or broad singlet at 1.0–1.5 ppm, and in particular by its typical high-field ^{13}C NMR signal in the region around -6 to -16 ppm, slightly downfield from those of the cationic sulfene complexes $[(\text{C}_5\text{H}_5)\text{Ru}(\text{P-P})(\text{CH}_2\text{SO}_2)]^+$ (-16 to -22 ppm).^{9,11} Spin–spin coupling with the two nonequivalent phosphorus nuclei is only small and was not resolved. Other characteristic features are the $\nu(\text{SO})$ absorptions in the infrared spectra and, for the tungsten complexes, surprisingly small ^{183}W – ^{31}P couplings. The latter is a clear indication of the presence of a strongly π -bonding η^2 ligand.²⁰ Indeed, as judged from the high frequency of the CO stretching vibrations, the sulfene ligand surpasses typical π -acceptor ligands such as maleic anhydride,²¹ CS, CS_2 ,²² or even SO_2 in its ability to take up electron density from the metal.

The structure of **10a** was determined by X-ray crystallography; Figure 3 shows an ORTEP diagram.

The tungsten atom resides in the center of a distorted pentagonal bipyramid with the sulfene ligand occupying two adjacent sites. The largest angle deviations within the pentagonal base are associated with the three-membered W–S–C ring and the vicinity of the bulky phosphine ligand. The two W–P bonds are almost equal in length and marginally shorter than in the SO_2 complex **8b**, but the W–S bond is 0.1 Å longer than that in **8b**. The W–C(5) distance compares well with the length of metal–carbon bonds in tungsten–alkene complexes.²³

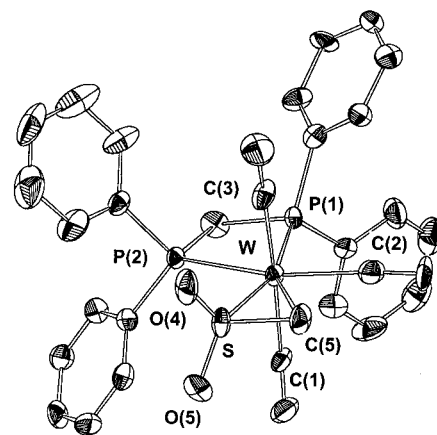


Figure 3. ORTEP plot of *mer*- $[\text{W}(\text{CO})_3(\text{dppm})(\text{CH}_2\text{SO}_2)]$ (**10a**).

Discussion

The synthesis of the sulfur dioxide complexes **5–8** as outlined in eqs 1 and 2 exploits the well-known reactivity of nitrile derivatives of the chromium group carbonyls.²⁴ The facial intermediates **5** and **6** are thermodynamically less stable than their meridional isomers **7** and **8**. In the latter, the LUMO of the strongly π -accepting ligand SO_2 can interact with a high and largely metal-centered HOMO (d_{xy} if the *trans*- $\text{M}(\text{CO})_2$ unit is taken as defining the z axis) which is stabilized by π bonding to only one carbonyl ligand. The isomerization is expected to proceed via some form of intramolecular twist mechanism²⁵ which on the way to the transition state requires a considerable compression of some of the bond angles around the central metal atom. This would offer a ready explanation why the bis(diphenylphosphino)ferrocene complexes **5e** and **6e** with their relatively large and inflexible P–M–P angles^{14c,26} are reluctant to isomerize.

The reaction of the SO_2 complexes with diazomethane is smooth and selective. Analogy with the formation of the cationic ruthenium sulfene complexes⁹ (Scheme 4) suggests that also in the present case the methylene transfer is initiated by nucleophilic attack at sulfur. Nucleophilic additions to cationic SO_2 complexes are well-documented.^{10,27,28} Uncharged complexes of sulfur dioxide, however, and notably those of the chromium group, react with nucleophiles with substitution of either SO_2 or other labile ligands.^{12,17,19} There appear to be only two reported cases of nucleophilic addition to neutral SO_2 complexes, one involving the formation of a platinum–sulfine complex from $[\text{Pt}(\text{PPh}_3)_3(\text{SO}_2)]$,²⁹ and the

- (18) (a) Appleton, D. G.; Clark, H. C.; Manzer, L. E. *Coord. Chem. Rev.* **1973**, *10*, 335–422. (b) Shustorovich, E. M.; Porai-Koshits, M. A.; Buslaev, Y. A. *Coord. Chem. Rev.* **1975**, *17*, 1–98.
- (19) Shen, J.-K.; Kubas, G. J.; Rheingold, A. L. *Inorg. Chim. Acta* **1995**, *240*, 99–104.
- (20) Schenk, W. A.; Buchner, W. *Inorg. Chim. Acta* **1983**, *70*, 189–196.
- (21) Schenk, W. A.; Müller, H. *Chem. Ber.* **1982**, *115*, 3618–3630.
- (22) Schenk, W. A.; Schwietzke, T.; Müller, H. *J. Organomet. Chem.* **1982**, *232*, C41–C47.

- (23) (a) Grevels, F. W.; Lindemann, M.; Benn, R.; Goddard, R.; Krüger, C. *Z. Naturforsch., B* **1980**, *35*, 1298–1309. (b) Berke, H.; Huttner, G.; Sontag, C.; Zsolnai, L. *Z. Naturforsch., B* **1985**, *40*, 799–807. (c) Grevels, F. W.; Jacke, J.; Betz, P.; Krüger, C.; Tsay, Y. H. *Organometallics* **1989**, *8*, 293–298.
- (24) (a) Tate, D. P.; Knipple, W. R.; Augl, J. M. *Inorg. Chem.* **1962**, *1*, 433–434. (b) Kubas, G. J. *Inorg. Chem.* **1983**, *22*, 692–694.
- (25) (a) Rodger, A.; Johnson, B. F. G. *Inorg. Chem.* **1988**, *27*, 3061–3062. (b) Wilkins, R. G. *Kinetics and Mechanism of Reactions of Transition Metal Complexes*, 2nd ed; VCH: Weinheim, 1991; p 343–354.
- (26) Bandoli, G.; Dolmella, A. *Coord. Chem. Rev.* **2000**, *209*, 161–196.
- (27) Schenk, W. A. *Angew. Chem.* **1987**, *99*, 101–112; *Angew. Chem., Int. Ed. Engl.* **1987**, *26*, 98–109.
- (28) Kubas, G. J. *Acc. Chem. Res.* **1994**, *27*, 183–190.
- (29) Götzfried, F.; Beck, W. *J. Organomet. Chem.* **1980**, *191*, 329–338.

other one describing the addition of methoxide ion to the cluster $[\text{Ir}_4(\text{CO})_{11}(\mu\text{-SO}_2)]$.³⁰

The stability of the sulfene complexes depends largely on the electron density at the metal and the ability of the metal complex fragment to engage in π -back-bonding. For example, in the ruthenium series the complexes $[(\text{C}_5\text{H}_5)\text{Ru}(\text{P-P})(\text{CH}_2\text{SO}_2)]\text{PF}_6$ are quite labile and have to be handled at low temperature, while $[(\text{C}_5\text{Me}_5)\text{Ru}(\text{PMe}_3)_2(\text{CH}_2\text{SO}_2)]\text{PF}_6$ is a perfectly stable compound.⁹ Indeed, all attempts to convert the less electron-rich complexes $[\text{W}(\text{CO})_4(\text{PR}_3)(\text{SO}_2)]$ ^{12a} into analogous sulfene complexes have failed and lead only to intractable mixtures of decomposition products. The higher stability of the tungsten complexes **10a–e** compared to their molybdenum analogues **9a–d** is in line with previous experience with tungsten carbonyl–alkene complexes, which undergo dissociative ligand exchange reactions much slower than the corresponding molybdenum compounds.^{21,31}

A comparison of the bond lengths of the sulfene complexes with those in uncoordinated sulfene and in thiirane *S,S*-dioxide reveals some interesting aspects (Figure 4).

The C=S double bond in sulfene (as calculated by ab initio-SCF methods)³² is very short. This is undoubtedly due to the contraction of the valence orbitals at sulfur caused by the two electronegative oxygen substituents. Upon coordination to the cation $[(\text{C}_5\text{Me}_5)\text{Ru}(\text{PMe}_3)_2]^+$ the C–S distance increases by more than 0.1 Å^{9b} as a result of electron donation into the LUMO of the CH_2SO_2 ligand. Apparently the degree of back-donation is even larger in the neutral complex **10a** where the C–S bond length has increased to

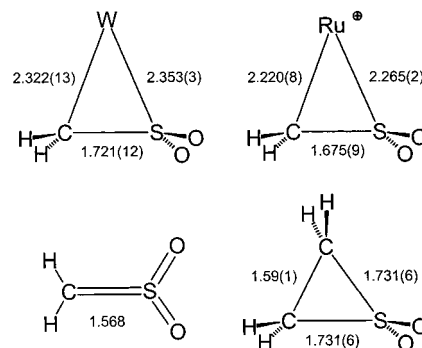


Figure 4. Comparison of bond lengths (Å) of *mer*- $[\text{W}(\text{CO})_3(\text{dppm})(\text{CH}_2\text{SO}_2)]$ (**10a**), $[(\text{C}_5\text{Me}_5)\text{Ru}(\text{PMe}_3)_2(\text{CH}_2\text{SO}_2)]\text{PF}_6$,^{9b} sulfene,³² and thiirane *S,S*-dioxide.³³

1.72 Å, comparable to the single bond in thiirane *S,S*-dioxide.³³ The net result is a remarkable stability of the sulfene complexes *mer*- $[\text{M}(\text{CO})_3(\text{P-P})(\text{CH}_2\text{SO}_2)]$, particularly for $\text{M} = \text{W}$. The molybdenum complexes nevertheless tend to release the sulfene ligand under mild conditions and may thus provide a ready source of sulfene. Work along these lines is in progress in our laboratory.

Acknowledgment. This work was generously supported by the Deutsche Forschungsgemeinschaft (SFB 347) and the Fonds der Chemischen Industrie.

Supporting Information Available: Three X-ray crystallographic files, in CIF format. This material is available free of charge via the Internet at <http://pubs.acs.org>.

(30) Braga, D.; Ros, R.; Roulet, R. *J. Organomet. Chem.* **1985**, 286, C8–C12.

(31) Schenk, W. A.; Müller, H. *Inorg. Chem.* **1981**, 20, 6–8.

(32) Block, E.; Schwan, A.; Dixon, D. A. *J. Am. Chem. Soc.* **1992**, 114, 3492–3499.

IC010963E

(33) Nakano, Y.; Saito, S.; Morino, Y. *Bull. Chem. Soc. Jpn.* **1970**, 43, 368–371.